Optically Active Polyethers. 1. Studies of the Crystallization in Blends of the Enantiomers and the Stereoblock Form of Poly(epichlorohydrin)†

K. L. Singfield and G. R. Brown*

Department of Chemistry, McGill University, Montréal, Québec, Canada H3A 2K6

Received May 16, 1994; Revised Manuscript Received November 8, 1994®

ABSTRACT: The isothermal crystallization kinetics and morphology of the melt-crystallized optically active polyenantiomers, their blends, and the stereoblock form of poly(epichlorohydrin) have been investigated using polarized light video microscopy. The optically active polyenantiomers develop regularly banded spherulites, while the equimolar blend and the stereoblock polymer form nonbanded, coarser spherulites. The apparent morphological differences among the polymers suggest a stereospecific segregation at the growth front in an attempt to produce optically pure lamellae. The equilibrium melting temperature as determined by the classical Hoffman−Weeks method was found to be 411 ± 1 K for all of the polymers. Over the range of crystallization temperatures from the T_g (247 K) to $T_m°$, the spherulite radial growth rates of the 50:50 blend of the polyenantiomers are depressed relative to those of either of the optically pure components. A further marked reduction in growth rates is recorded for the stereoblock polymer. An analysis of the linear spherulite radial growth rates in terms of the Hoffman−Lauritzen treatment gave evidence of the development of larger folds, hence a rougher lamellar surface in the stereoblock polymer than in the polyenantiomers.

Introduction

Optically active polymers are the subject of an increasing number of studies, particularly since equimolar binary blends of the optically active polyenantiomers have been shown to behave differently from their component polyenantiomers.[1−8] Much of this attention has been focused on the stereocomplexation of the polyenantiomers. The term stereocomplexation, although originally used to describe specific interactions between stereoregular isotactic and syndiotactic poly(methyl methacrylate) chains,[9] has been adopted more widely to describe the stereoselective association between optically active enantiomorphic macromolecules during crystallization. The resulting racemic nature of the stereocomplex allows for closer packing of the chains so that the racemic crystallites are often significantly more stable toward melting than the optically active polyenantiomer crystallites.

Ikada et al.[8] have demonstrated that at various blend ratios, the polyenantiomers of optically active poly(lactic acid) form stereocomplexes both from the melt and solution, resulting in racemic crystallites with side-by-side packing of the polyenantiomers. The crystal structure of the stereocomplex was determined by Okihara et al.[10] to be composed of a triclinic racemic unit cell with lateral packing of left-handed 3_1 helices of one polyenantiomer and right-handed helices of the other. By comparison, the optically active polyenantiomers crystallized with unique handedness having a 10_3 helix configuration in the pseudo-orthorhombic α-form,[11−13] although a less stable β-form was composed of 3_1 helices. The stereocomplex melted at a temperature 50 degrees higher than that of the α-form. Similar behavior has been reported by Prud'homme et al.[1−6] for the optically active forms of poly(α-methyl-α-ethyl-β-propiolactone). The crystalline stereocomplex, formed both from solution and from the melt, possessed a lattice structure different from that of either component polyenantiomer, and melted at a temperature approximately 40 degrees higher than either component polyenantiomer. In binary blends of the polyenantiomers and in ternary blends which included the racemic polymer, the stereocomplex was formed preferentially and controlled the morphology.

Because both chiral monomers are only rarely available for polymerization, the separate polyenantiomers are seldom available for blending. Dumas et al.[14] used a stereoselective mechanism in the polymerization of racemic monomer to prepare poly(*tert*-butylthiirane) composed essentially of a statistical mixture of *R* and *S* polyenantiomer chains. The racemic mixture was more stable toward melting than the optically active *R* polyenantiomer, with a 40 degrees difference in the melting temperature. It was later concluded from X-ray diffraction studies[15] that the optically active polyenantiomer crystallizes in a trigonal crystal lattice composed of three right-handed 3_1 helices with statistical up and down packing, while the racemic polymer mixture cocrystallizes in a monoclinic crystal lattice. Similarly, based on an analysis of the X-ray diffraction patterns, Sakakihara et al.[16] concluded that poly(*tert*-butylethylene oxide) prepared from racemic monomer via a stereoselective mechanism crystallizes in a tetragonal crystal lattice with an optically inactive unit cell. Two right-handed *S* helices and two left-handed *R* helices pass through the unit cell, existing as a random mixture of upward and downward helices in a 1:1 ratio. Since neither optically active polyenantiomer was available, comparison of thermal stability or crystal structure was not made.

The phenomenon of stereocomplexation is not universal among mixtures of optically active polymers. Yokouchi et al.[17] and Okamura et al.[18] have independently reported that the X-ray diffraction pattern of naturally occurring optically active i-poly(β-hydroxybutyrate) (PHB) is indistinguishable from that of isotactic PHB polymerized from the racemic monomer using a stereoselective catalyst. It was concluded that

* To whom correspondence should be addressed.

† Presented in part at the 76th CSC Conference, Sherbrooke, Québec, Canada.

® Abstract published in *Advance ACS Abstracts,* January 15, 1995.

0024-9297/95/2228-1290$09.00/0

the racemic polymer crystallizes into two kinds of optically pure crystallites, i.e., with so-called intercrystallite optical compensation:[19] crystallites (lamellae) composed of only left-handed helices of *R* chains and those of only right-handed helices of *S* chains. The optically pure *R* polymer develops crystallites composed of left-handed helices only. More recently, Bloembergen et al.[20,21] have reported that physical properties of a synthetic highly stereoregular form of i-PHB corresponded closely to that of the naturally occurring optically active polymer. A stereoblock model was proposed with stereoregular right-handed and left-handed helical segments of the chains contained in separate crystalline domains, i.e., an intercrystallite optical compensation. In a similar study, Yokouchi et al.[22] also deduced an intercrystallite compensation for racemic poly(β-ethyl-β-propiolactone) prepared with a stereoselective catalyst although no comparison was made with the optically active polyenantiomer.

Sakakihara et al.[19] polymerized the racemic propylene sulfide monomer with a stereoselective catalyst and optically pure monomer with another coordinate-type catalyst. X-ray diffraction studies suggested that these polymers have the same crystal structures as evidenced by identical fiber photographs. However, the optically pure homopolymer was slightly more thermally stable. Yet, it was concluded that the racemic polymer possesses an intercrystallite optical compensation. Takahashi et al.[23] have also reported that racemic poly(isopropylethylene oxide) crystallizes with an intercrystallite optical compensation.

Although the crystal structure of optically active poly(propylene oxide) has not yet been reported, several descriptions have been given of the X-ray diffraction pattern of isotactic poly((*R*,*S*)-propylene oxide).[24-27] On the basis of their studies of poly(propylene oxide) prepared with a catalyst that is known to be stereoselective, Cesari et al.[27] described the crystal lattice as $P2_12_12_1$, a space group requiring optically pure unit cells with up and down packing of the helices,[26] without any mention of helix sense. On the basis of the results of this study, others[10] have subsequently included poly(propylene oxide) in the list of polymers unable to form racemate complexes, i.e., stereocomplexes. Several authors[28-31] have investigated the crystal structure of the isotactic poly((*R*,*S*)-epichlorohydrin) prepared with coordinate-type catalysts. Richards[28] has reported an orthorhombic unit cell with dimensions of $a = 12.16$ Å, $b = 4.90$ Å, and $c = 7.03$ Å, with two possible space groups, $P2_12_12_1$ and $Pna2_1$.

Despite the growing interest in optically active polymers, little attention has been directed toward the kinetics of the crystallization in blends of these chiral species. Any stereoselection/rejection processes that occur during crystallization should manifest their effect clearly in the kinetics. Indeed, in his work on poly(propylene oxide), Magill[32] found that the optically active poly((*S*)-propylene oxide) displays overall faster spherulite growth rates than the racemic isotactic polymer. In a study of a series of crystalline poly((*R*,*S*)-epichlorohydrin) polymers with varying degrees of optical activity, Dreyfuss[33] described two types of spherulites, type I and type II, the latter possessing a finer fibrillar structure and only in rare cases displaying a banded morphology. Occasionally, both forms could be seen in the same spherulite. Type II spherulites were observed to melt at a slightly higher temperature, crystallized more rapidly, and had some optical activity. It was concluded from this qualitative study that type II spherulites were formed from optically active polymer sequences while type I spherulites were formed from racemic polymers with little or no optical activity.

The present investigation is the first report of poly(epichlorohydrin) prepared from the pure enantiomers. It is unique in comparing the crystallization kinetics of the two opposite polyenantiomers of epichlorohydrin, their blends, and the corresponding stereoblock polymer. Polymerization of either enantiomer of epichlorohydrin with a coordinate-type catalyst yields the isotactic optically pure polyenantiomer with true asymmetric carbon centers along the polymer backbone. The racemic monomer is also readily polymerized and generates a large fraction of crystalline, isotactic polymer with long stereoregular sequences. By use of polarized light microscopy, Zmudzinski et al.[31] have shown previously that the spherulitic radial growth rates of partially crystalline isotactic poly((*R*,*S*)-epichlorohydrin) are sufficiently slow to permit the quantitative measurement over the entire range of temperatures from above the glass transition temperature (T_g) to the melting temperature, with a maximum value in the vicinity of 330 K. The work described in this paper was performed with the aim of developing a better understanding of the crystallization mechanisms which govern the growth of polymer spherulites from the melt through the study of the crystallization kinetics of the optically active forms of poly(epichlorohydrin) and their blends as well as the stereoblock polymer. It was of particular interest to determine the extent to which cocrystallization of polyenantiomers could occur and the effects of polyenantiomer segregation on the rates of crystallization.

Experimental Section

Materials. Racemic epichlorohydrin monomer [99+% Aldrich] was distilled before use and then polymerized according to the method of Vandenberg, using $Et_3Al{\cdot}0.6H_2O$, as the initiator.[34] The polymer was fractionated into its atactic and isotactic (designated i-P*RS*ECH) components, as described previously.[34] Polymerization of the optically active monomers (*R*)-(−)-epichlorohydrin [99% Aldrich] and (*S*)-(+)-epichlorohydrin [99% Aldrich] (as received) under the same conditions used for the racemic monomer resulted in a high conversion (>90%) of isotactic, optically pure polymers (designated P*R*ECH and P*S*ECH, respectively) that did not require fractionation. The weight average molecular weights of the polymers, determined by gel permeation chromatography at 323 K, in THF, using a Varian D6-600 G.P.C. having a Varian (Model RI-4) refractive index detector, were found to be 450 000, as interpreted using polystyrene standards and application of a *Q* factor of 25. The polymers were found to have a unimodal, relatively narrow molecular weight distribution (polydispersity of 1.6 for both P*R*ECH and P*S*ECH and 1.4 for the i-P*RS*ECH).

Figure 1 contains the expanded methylene region of the ^{13}C NMR spectra of the isotactic poly((*R*,*S*)-epichlorohydrin) and the optically active P*R*ECH. The spectra were recorded on a Varian Unity 500 NMR spectrometer operating at 125 MHz at 323 K using 5−10 wt % polymer solutions prepared with deuterated dimethyl sulfoxide. The pulse angle for these experiments was 70° with a 1 s acquisition time and a 2 s delay time, and the number of transients was equal to 16 000. The assignments of the fine structure resonances are based on the interpretational scheme of Cheng and Smith[35] for regioregular poly((*R*,*S*)-epichlorohydrin). The absence of inverted sequences (regioirregularities resulting from head-to-head or tail-to-tail additions of monomer) in any of these polymers is consistent with previous reports[35-38] and confirms that during the polymerization of optically active epichlorohydrin by the Vanderberg method only one of the C−O bonds of the asymmetric monomer ring is subject to cleavage. On the basis of

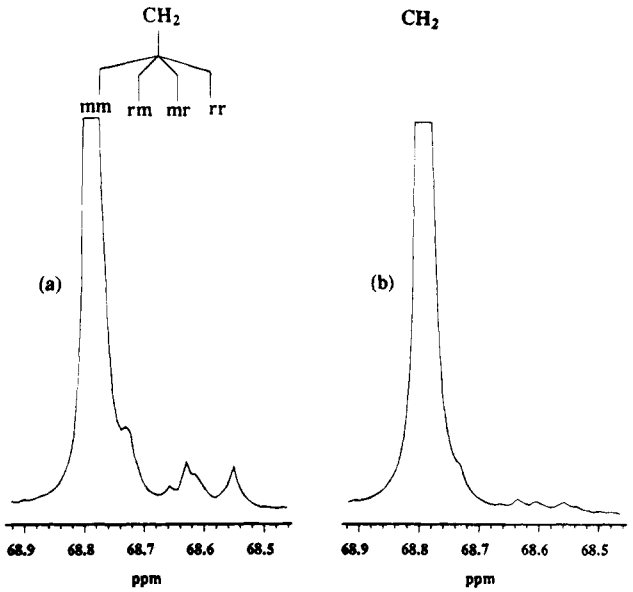

Figure 1. Expanded methylene carbon region of the ^{13}C NMR spectra of (a) i-*PRS*ECH stereoblock and (b) optically active *PR*ECH.

the relative peak areas at 68.55, 68.63, and 68.73 ppm to that at 68.78 ppm the stereoirregularities manifested in the spectrum of i-*PRS*ECH make up no more than 3% of the polymer chain. These are attributed to junctions or defect sites, between long stereoregular sequences, and not to a separate atactic chain fraction. Essentially, the i-*PRS*ECH polymer can be described as a stereoblock polymer. Assuming a random occurrence of defect sites along the polymer chain, the average length of a stereosequence is estimated to be 33 monomer units.

Blends of different ratios of *PS*ECH and *PR*ECH were made by dissolving the appropriate amounts of each polymer in tetrahydrofuran (THF) at 323 K for several hours with stirring under a nitrogen atmosphere. The THF solvent was prepurified by refluxing and distilling over sodium benzophenol. Cold, anhydrous diethyl ether was used to precipitate the blend from the 1 wt % polymer solutions with vigorous stirring. The polymers with dried *in vacuo* for at least 2 weeks prior to analysis. All of the polymers were stored under vacuum and were used without the addition of antioxidant.

Polarized Light Microscopy. The samples were prepared for viewing by first pressing the polymer between two circular glass coverslips on a hot plate at 448 K until the polymer just melted. The samples were then transferred to a hotstage and melted for 15 min at 448 K under a nitrogen atmosphere, cooled at a nominal rate of 130 °C/min to the selected isothermal crystallization temperature and held constant to within ± 0.1 deg. Sample thickness was controlled by the use of 12 μm thick aluminum foil spacers. Only samples of 10–20 μm thickness were employed. Typically, one polymer sample was used to determine the growth rates G at three different crystallization temperatures when the undercoolings were ≥53 deg, but for smaller undercoolings a sample was used only once.

The crystallization behavior of the spherulites was followed by polarized light videomicroscopy using a Nikon Optiphot-Polarized light microscope in tandem with a Linkam THMS600 hotstage, TMS91 temperature controller, and CS196 cooling unit, as described previously.[39] A COHU vide camera mounted on the microscope transmitted real-time images through a computer to a secondary monitor (Electrohome RGB) for display. The computer housed a frame-grabber (PCVisions Plus) to digitize the analog signal. These images were simultaneously recorded onto videotape using a Mitsubishi U80 video cassette recorder for later analysis. A video analysis software program (JAVA, Jandel Scientific) was used to measure the radii of three spherulites in the field at six regular time intervals well before impingement during the isothermal crystallization. The radius of each spherulite was taken as the average of 12–16 measurements. The slope of the resultant straight line ($r^2 \geq 0.999$) plot of radius as a function of time was taken as the radial growth rate, G. Polarized light photomicrographs were taken with a 35 mm Nikon camera mounted in place of the video camera.

Differential Scanning Calorimetry, DSC. The basic thermal behavior of each polymer was studied by DSC using a Perkin-Elmer DSC-7 instrument, calibrated for temperature and peak area using indium and octadecane standards. To determine the glass transition temperature the samples were first melted at 448 K for 15 min before they were quench-cooled to 213 K and then heated at a scanning rate of 10 °C/min. Analysis of each of the polymers yielded a common T_g value of 247 K. Isothermal crystallizations were performed with each polymer for the construction of a so-called Hoffman–Weeks plot of the observed melting temperature as a function of crystallization temperature which was used to determine the equilibrium melting temperature, $T_m°$. The samples were premelted at 448 K for 15 min, quench-cooled to the crystallization temperature, and held there for 24 h. The samples were then heated at a scanning rate of 20 °C/min and the melting temperature was taken as the maximum of the high temperature endotherm. A fresh sample was used for each crystallization.

WAXS Analysis. Nonoriented thin films were made by first pressing the polymer between two microscope slides lined with Teflon on a hotplate at 448 K until the polymer melted. The polymer assembly was then quickly transferred to a Mettler FP52 hotstage at the same temperature with a nitrogen stream passing over the sample. It was kept at this temperature for 20 min and then cooled slowly to 333 K at which temperature it remained for 1 h. The film was then removed from the Teflon-lined slides and annealed *in vacuo* at 353 K for 15 h. X-ray powder diffraction patterns were obtained with a flat film Warhus camera using nickel-filtered Cu Kα radiation. Sodium fluoride was used as the calibration standard.

Results and Discussion

WAXS Analysis. As a first approximation, the X-ray powder diffraction patterns of the optically active *PR*ECH and *PS*ECH, their 50:50 blend, and the stereoblock i-*PRS*ECH are the same. Figure 2 shows a series of diffraction rings for each polymer. The relative intensity and spacings of the rings are consistent with the most intense reflections recorded for isotactic poly((*R*,*S*)-epichlorohydrin) by Richards.[28] A narrow diffraction line width superimposed on the background intensity indicates a degree of order in the i-*PRS*ECH crystals which is comparable to that of the other polymers.

Melting Behavior. Upon rapid cooling of the melt from 448 to 213 K all of the polymers were essentially amorphous. During subsequent heating, at a scanning rate of 20 °C/min, both of the polyenantiomers and their 50:50 blend displayed a single crystallization exotherm at 313 K that on continued heating yielded a single melting endotherm at 385 K. For the stereoblock i-*PRS*ECH, the corresponding exotherm and endotherm values shifted to 323 and 379 K, respectively.

In Figure 3 the DSC heating thermograms of the polymers crystallized for 24 h at 373 K are presented. Under these conditions all of the polymers exhibit a double melting peak endotherm, suggesting multiple degrees of crystal size, perfection, and/or internal order. Janeczek et al.[40] have previously identified multiple melting endotherms in isotactic poly((*R*,*S*)-epichlorohydrin), with the lower melting peak shifting to higher temperatures when the polymer was crystallized at temperatures >333 K. In the present study, the melting

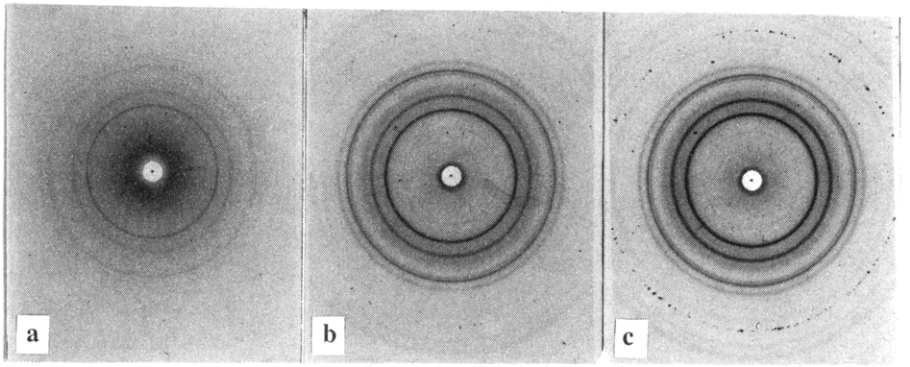

Figure 2. X-ray powder diffraction patterns of (a) the stereoblock i-P*RS*ECH, (b) the optically active P*R*ECH and P*S*ECH, and (c) the 50:50 blend of the polyenantiomers. Diffraction spots are due to the calibration standard.

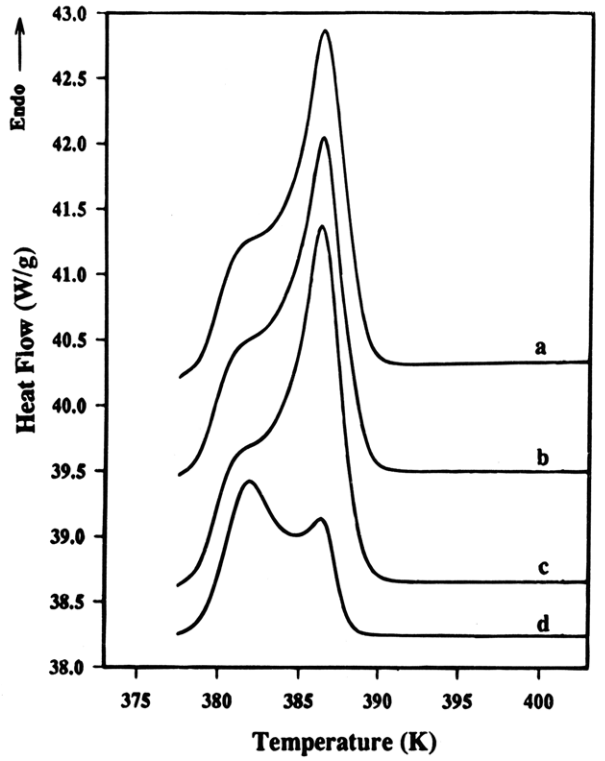

Figure 3. DSC heating thermograms of (a) the optically active P*S*ECH, (b) the optically active P*R*ECH, (c) the 50:50 blend of the polyenantiomers, and (d) the stereoblock i-P*RS*ECH; crystallized at 373 K for 24 h and scanned at a heating rate of 20 °C/min.

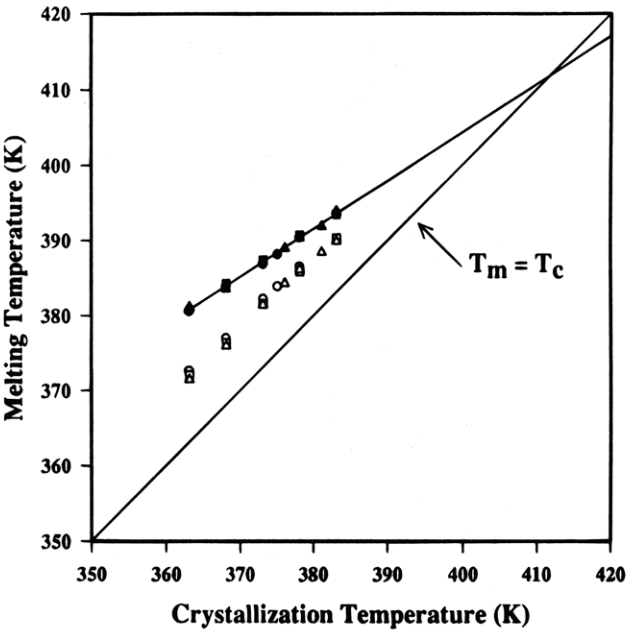

Figure 4. Hoffman–Weeks plot of the observed melting temperature as a function of crystallization temperature for optically active P*R*ECH and P*S*ECH (▲), the 50:50 blend of the polyenantiomers (■), and the stereoblock i-P*RS*ECH (●). The hollow symbols represent the corresponding lower melting endotherm maxima.

endotherms of the stereoblock polymer, i-P*RS*ECH, consistently indicated a smaller population of the higher melting crystals than that in either polyenantiomer or the 50:50 blend. However, both melting peak maxima coincided for all of these polymers when crystallized at temperatures above 363 K for 24 h. In general, the i-P*RS*ECH stereoblock polymer produced a wider population of crystals less stable against melting but an annealing at higher temperatures increased the stability of the crystals.

The equilibrium melt temperature, $T_m°$, was determined according to the method of Hoffman and Weeks,[41] by extrapolation of the data in Figure 4. The colinearity of the melting point data led to a common $T_m°$ value of 411 ± 1 K for all of the polymers.

Morphology. Isotactic poly(epichlorohydrin) crystallizes from the melt readily forming spherulites with the characteristic Maltese extinction cross visible under a polarized light microscope with crossed polars. In addition, the spherulites of the optically active P*R*ECH and P*S*ECH exhibit periodic birefringent extinction rings, or bands, when the crystallization temperature exceeds the temperature of maximum growth rate (T_{max}). The polarized light photomicrographs in Figure 5 illustrate this morphology, capturing spherulites of the different polymers used in this study during isothermal crystallization at 353 K.

The presence of banding is common in many polymer spherulites with the size of the extinction interval, or bandwidth, increasing with temperature.[32,42–52] It is generally ascribed to a twisting of crystallographic orientation about radii that apparently reflects a cooperative twisting of radiating lamellar crystals about their axes of fastest growth, and implies a high degree of coordination in the packing of the lamellae.[47] Polarized light microscopy and light scattering studies of banded spherulites have assigned the observed extinction bands and diffraction rings to the helicoidal orientation of the crystals within the spherulites.[50,51] Similar work has correlated the periodicity of the extinction bands with X-ray microdiffraction and electron diffraction patterns of the banded and nonbanded areas of the spherulite, presenting direct evidence for lamellar twisting.[43,44] Most recently, Briber and Khoury[53] have

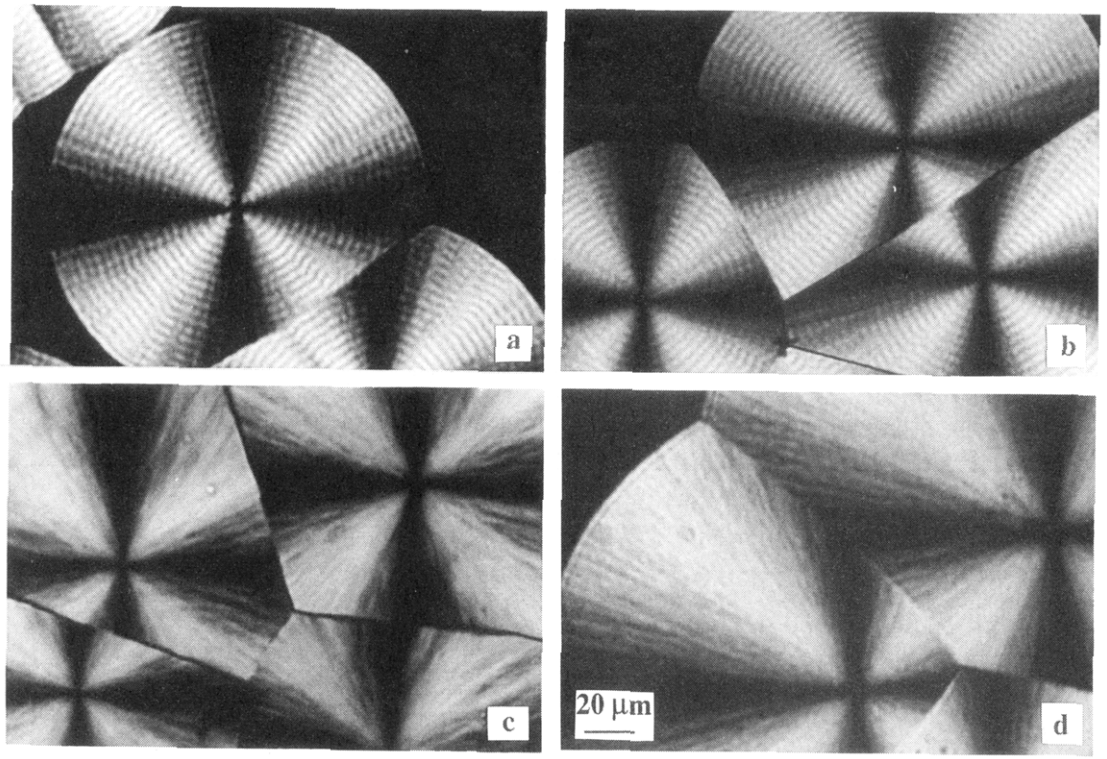

Figure 5. Polarized light photomicrographs of spherulites of (a) optically active P*R*ECH, (b) optically active PSECH, (c) the stereoblock i-P*RS*ECH, and (d) the 50:50 blend of the polyenantiomers; crystallized at 353 K.

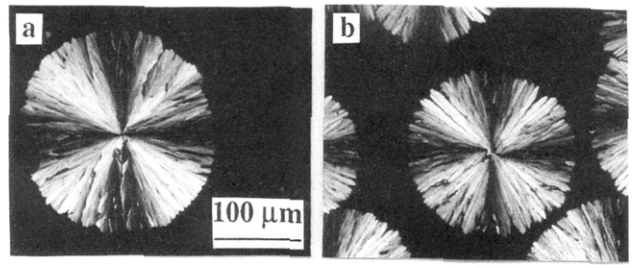

Figure 6. Polarized light photomicrographs of spherulites of (a) the 50:50 blend of the polyenantiomers and (b) the stereoblock i-P*RS*ECH; crystallized at 353 K.

reported a unique type of banded morphology in crystalline poly(vinylidene fluoride), PVF_2, the minor component crystallized from a binary blend with a noncrystalline polymer. The banding periodicity in the spherulites corresponded to the spatial periodicity of a particular twisting/splaying growth motif in the radial direction.

Interestingly, the stereoblock i-P*RS*ECH produced no evidence of banded spherulites at any crystallization temperature. Instead, the spherulites appeared to have a coarser, more open texture than those of the optically active polymers, as shown in Figure 6 for spherulites developed in the thin sample section. The apparent effect of the defect sites in the stereoblock i-P*RS*ECH polymer is to disrupt the regularity of the chain to a sufficient extent that any regular twisting of the lamellae is inhibited at all crystallization temperatures. These observations are in keeping with those of Magill[32] who reported a banded spherulite appearance for optically active i-poly((*S*)-propylene oxide) while only in very rare instances did he observe extinction bands in spherulites of the corresponding racemic i-poly((*R*,*S*)-propylene oxide). The morphological differences between the optically pure and the stereoblock polymers reflect those reported by Dreyfuss.[33]

The banding and general morphology of spherulites of a 95:5 blend of the polyenantiomers were indistinguishable from those of either optically active component at the same crystallization temperature. If this 5% addition is considered an "impurity" in the otherwise pure homopolymer system, the insensitivity with respect to spherulite morphology is in contrast with the dramatic effect of the lesser 3% defect site "impurity" in the stereoblock polymer which displays coarse, open spherulites. This is consistent with a stereoblock structure and emphasizes the important role that these defects play in the crystal growth.

Periodic extinction bands were also observed in the spherulites of a 70:30 or 30:70 blend of the polyenantiomers; but as Figure 7 illustrates, the band periodicity is larger than that of the spherulites of the optically active polyenantiomer at a given temperature. Finally, at a polyenantiomer blend ratio of 50:50, the effect of one polyenantiomer on the other is to abolish lamellar twisting, as evidenced by unbanded spherulites at all crystallization temperatures. The effect of blending of the polyenantiomers on the spherulite morphology is to make the spherulites more open,[54] increasing the size of the bands, and to apparently hinder the twisting of lamellae that occurs naturally at a given crystallization temperature, or else to relieve the stress which causes the lamellae to twist.[51,55,56] The apparent morphological differences among the polymers suggest a stereospecific segregation at the growth front in an attempt to produce optically pure lamellae. In the 50:50 blend this mechanism would induce branching of the lamellae with the rejection of opposite sense chains, thus inhibiting a regular twisting of the lamellae. A similar mechanism can occur during the crystallization of the stereoblock i-P*RS*ECH polymer and would involve the rejection of stereoregular segments of the chain. This type of growth front stereospecific segregation would be manifested in the equimolar enantiomeric blend and in the

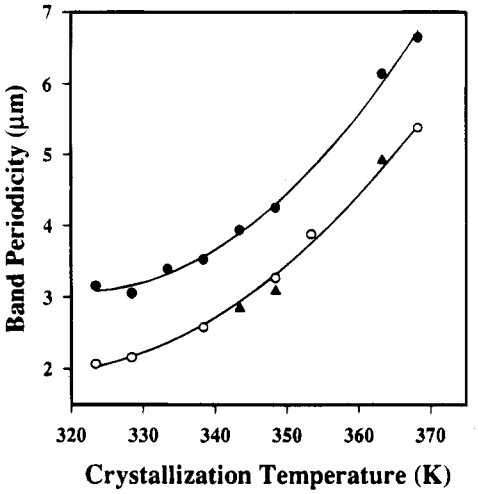

Figure 7. Relationship between the spherulite band periodicity and isothermal crystallization temperature for the optically active PRECH and PSECH (▲), the 95:5 blend of the polyenantiomers (○), and the 30:70 and 70:30 blend of the polyenantiomers (●). The data for the blends are fitted to a second-order regression. Band periodicity is taken as the combined light and dark intervals.

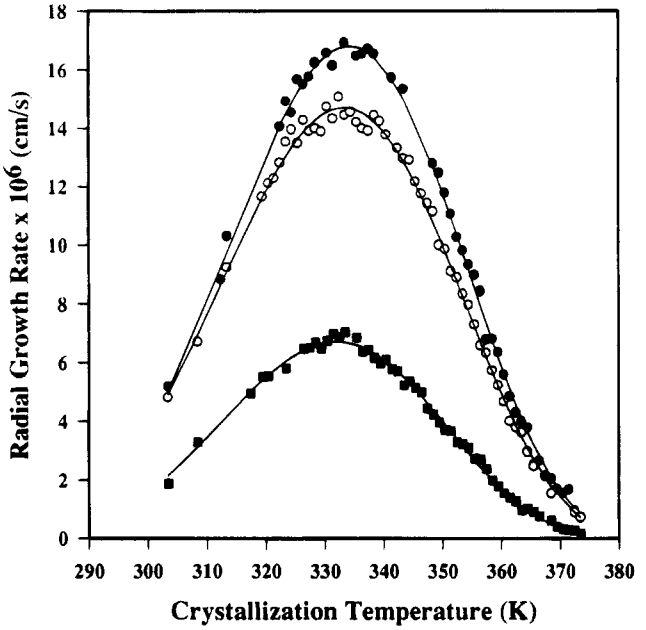

Figure 8. Plot of the spherulite linear radial growth rate dependence on isothermal crystallization temperature for the optically active PRECH and PSECH (●), the 50:50 blend of the polyenantiomers (○), and the stereoblock i-PRSECH (■). The solid line represents the best fit of the experimental data (symbols) to eq 1.

stereoblock as coarse, open spherulites. Since the stereoregular segments are covalently bound in the stereoblock polymer, branching would occur to a larger extent resulting in a coarser spherulite than in a 50:50 polyenantiomeric blend.

Spherulite Growth Rates. The spherulite radial growth rates of all of the polymers studied are presented in Figure 8 as a function of crystallization temperature. There is no difference between the growth rates of the optically active, stereoregular PRECH and PSECH polymers. The growth rates of the 50:50 blend of the polyenantiomers are depressed over a wide range of temperatures relative to those of the optically active systems. The entire crystallization curve for the stereoblock i-PRSECH polymer is markedly reduced relative to that of the stereoregular, optically active PRECH or PSECH polymers, and confirms sparse data presented for the poly((*R*,*S*)-epichlorohydrin) previously.[31] For all of the polymers the maximum in the growth rate occurs at the same crystallization temperature, T_{max}, equal to 336 K, corresponding to a T_{max}/T_m° ratio of 0.82, in excellent agreement with that found for other crystalline polymers.[57]

The experimentally determined growth rates were analyzed in terms of the Hoffman–Lauritzen treatment. The rate at which polymer spherulites grow in an isotropic medium can be described by the growth rate equation of the form:[58,59]

$$G = G_0(\Delta T)\exp\left[\frac{-U^*}{R(T_c - T_\infty)}\right]\exp\left[\frac{-K_g}{T_c(\Delta T)f}\right] \quad (1)$$

where G is the spherulite radial growth rate (cm/s), G_0 is the pre-exponential term, ΔT is the degree of undercooling ($T_m^\circ - T_c$), U^* is the activation energy for transport of crystallizable segments through the melt to the site of crystallization, R is the ideal gas constant, T_c is the isothermal crystallization temperature, T_∞ is the hypothetical temperature at which molecular motion associated with viscous flow ceases, K_g is the nucleation constant, and f is equal to $[2(T_c)/(T_m + T_c)]$. The constant K_g is further defined as $[jb_0\sigma\sigma_e T_m^\circ/k\Delta h_f]$, where the value of the regime coefficient, j, is equal to 4 in regimes I and III and 2 in regime II;[60] b_0 is the thickness of the crystallizing stem; σ and σ_e are the lateral and fold surface interfacial free energies, respectively; k is Boltzmann's constant; and Δh_f is the heat of fusion per unit volume of monomer units. The growth rate equation may be rewritten in logarithmic form:

$$\log G - \log \Delta T + \frac{U^*}{2.303R(T_c - T_\infty)} = \log G_0 - \frac{K_g}{T_c(\Delta T)f}$$

Plotting the left-hand side of the equation as a function of $1/T_c(\Delta T)f$ should give a straight line with an intercept equal to log G_0, and the product of lateral and fold surface interfacial free energies, $\sigma\sigma_e$, can be estimated from the slope, $-K_g$. In this analysis the experimentally determined values of T_m° and T_g were employed. The value of T_∞ was chosen by definition as $T_g - 30$ K.[58] There is no indication of a change in slope in the data plotted in Figure 9 that would correspond to a transition from regimes I to II or II to III. For these polymers, with this particular molecular weight, there is no evidence of a regime transition. Thus, the regime coefficient was chosen as 4. The spacing between the *110* planes of symmetry, equal to 4.56 Å,[28] was taken as b_0. From the unit cell density[28] and enthalpy of fusion data,[40] Δh_f was determined to be 2.11 erg/cm^3.

Table 1 contains the estimates of the parameters G_0, U^*, K_g, and $\sigma\sigma_e$ that result from the best fit of the data to the growth rate equation (1) by the procedures described previously.[39] The pre-exponential parameter, G_0, may be the most poorly defined parameter of the growth rate equation, mainly due to a general lack of growth rate data for polymers at large undercoolings. The observed differences in the estimates of G_0 reported in Table 1 are relatively small, as might be expected for similar polymers.

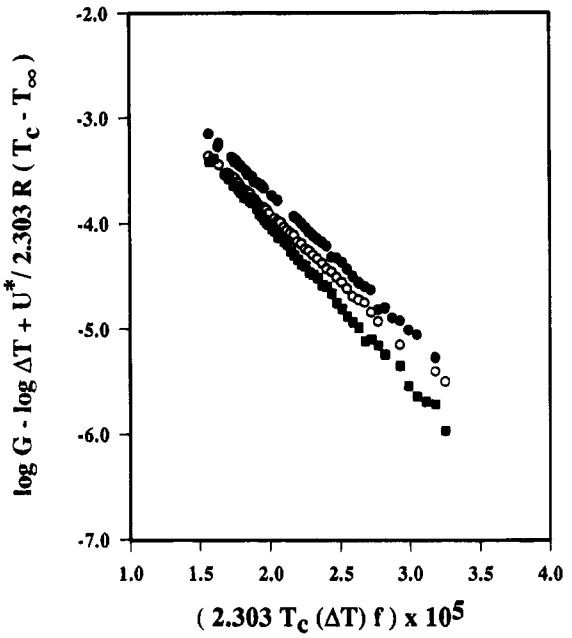

Figure 9. Plot of log G − log ΔT + $[U^*/2.303R(T_c - T_\infty)]$ against $1/T_c(\Delta T)f$ for optically active P*R*ECH and P*S*ECH (●), the 50:50 blend of the polyenantiomers (○), and the stereoblock i-P*RS*ECH (■); isothermally crystallized from the melt.

Table 1. Best-Fit Estimates of the Parameters in Equation 1

	G_0 (cm/s)	U^* (kJ/mol)	$10^{-4}K_g$ (K^2)	$\sigma\sigma_e$ (erg^2/cm^4)
stereoblock i-P*RS*ECH	0.12 ± 0.07	7.3 ± 0.3	15.5 ± 0.6	603
50:50 blend	0.04 ± 0.02	6.7 ± 0.2	12.6 ± 0.4	494
optically active P*R*ECH & P*S*ECH	0.07 ± 0.03	7.0 ± 0.3	12.8 ± 0.4	494

At large undercoolings, where transport processes are rate-controlling, the difference between the growth rates of P*R*ECH or P*S*ECH and those of their 50:50 blend gradually diminishes. This convergence of the growth rate curves is expected since the energy required to transport chains through an optically pure matrix is the same as that of the racemic blend. The best-fit estimate of the U^* parameter is essentially the same for P*R*ECH, P*S*ECH, their 50:50 blend, and the stereoblock i-P*RS*ECH and has a value of 7.0 × 10^3 J/mol. This calculated estimate is similar to the empirical universal value of 6280 J/mol suggested by Hoffman.[58] Since U^* reflects the mobility of the chains, which is governed by the value of T_g, its invariance among these polymer systems with identical glass transition temperatures is expected.

The calculated estimate of K_g is 12.7 × 10^4 K^2 for the optically active polymers and their 50:50 blend, but it is significantly larger for the stereoblock i-P*RS*ECH polymer, at 15.5 × 10^4 K^2. This difference is in accord with the suggestion presented above that the defect sites between stereoregular sequences of the i-P*RS*ECH chain interfere with the process of regular chain folding. Assuming that molecules attach themselves to growing crystals one segment at a time,[61] the growth will continue along the substrate until a defect site is encountered, at which time regular chain folding could be interrupted, or halted. In this case large chain loops and chain ends would develop and increase the free energy of the fold surface of the crystal. Moreover, since the native defect in the chain introduces an enantiomeric stereoregular segment, lateral crystal growth may be retarded as the substrate accommodates the new chain segment. This accommodation may be realized through branching or splitting which are mechanisms of spherulite development introduced by certain types of defects on crystal growth surfaces which can stop the lateral crystal growth.[62] Excessive branching or splitting of the lamellae would have a diminishing effect on the radial growth of the crystal, as is indeed observed.

The product $\sigma\sigma_e$ constitutes the distinction between the two K_g values given above. The major effect of the defect sites on growth rate may be gauged by measuring their contribution to the fold and lateral surface interfacial free energies. The product of the free energies is estimated at 603 erg^2/cm^4 for the stereoblock and 494 erg^2/cm^4 for the optically active polyenantiomers and their 50:50 blend. It is known that for a given polymer, the value of $\sigma\sigma_e$ increases with decreasing isotacticity, indicating an increase of roughness for both lateral and fold crystal surfaces.[63] Without an estimate of either component, however, it is impossible to assign a separate contribution to each term. Nevertheless, the value of σ is expected to be essentially constant for these systems so that the larger value reflects differences at the fold surface. Thus, these results suggest that the lamellae of the stereoblock polymer have a rougher surface than those of the optically active polyenantiomers and their blend due to the increased size and number of loops at the fold surface that are caused by the defect sites.

Summary and Conclusions

The individual polyenantiomers of poly(epichlorohydrin) displayed identical bulk crystallization and melting behavior and indistinguishable morphologies as well as growth rate kinetics. The bulk crystallization and melting behavior of each polyenantiomer and the 50:50 blend were the same under the conditions studied. The optically active polyenantiomers developed a banded spherulite morphology while the stereoblock i-P*RS*ECH polymer and the 50:50 blend of the polyenantiomers had unbanded, coarser, open spherulites. The radial growth rates of the 50:50 blend of the polyenantiomers were depressed over the entire range of crystallization temperatures relative to those of either optically active polyenantiomer. The radial growth rates of the stereoblock i-P*RS*ECH were markedly reduced compared to all of the polymers. A best-fit analysis of the observed growth rate data to the Hoffman–Lauritzen growth rate equation indicated a common rate of transport across the phase boundary for all of these polymers. However, the nucleation parameter, K_g, was greatest for the stereoblock i-P*RS*ECH polymer.

The relatively small reduction in the radial growth rates of the 50:50 blend of the polyenantiomers can be attributed to the rejection of chains of opposite sense at the growth front of stereospecific lamellae. A stereospecific segregation is expected to induce branching of the lamellae, thus inhibiting regular lamellae twisting and causing a coarse, open spherulite to develop. A similar mechanism can occur during the crystallization of the stereoblock i-P*RS*ECH polymer, involving the segregation of opposite sense stereoregular segments into stereospecific lamellae. As the stereoregular segments are covalently linked, the lamellae would be excessively branched and limited in their size. Again, the coarser, unbanded, open spherulites of the stereoblock polymer support this stereospecific segregation at the growth front. Indeed, the DSC heating thermo-

grams of i-*PRS*ECH from a quench-cooled melt state indicate that the crystals of the i-*PRS*ECH polymer are fewer, smaller, and less stable against melting than those of the optically active polyenantiomers or their 50:50 blend. Long anneals at high temperatures are perhaps sufficient to permit these long loops and chain ends of the rough surface to be incorporated into the crystal, thus increasing their stability. The influence of the defect sites in the stereoblock polymer is evidenced mainly through their contribution to the surface free energies in the crystal, which in turn is responsible for an increase in the value of the nucleation parameter, K_g. The growth rate is highly sensitive to changes in this exponent and the rates of crystallization of the i-*PRS*ECH polymer are consequently substantially less than those of the optically active polyenantiomers or their 50:50 blend, indicating the significant role of the defect site during crystal growth.

The results of this study suggest the formation of stereospecific lamellae in melt-crystallized spherulites of the 50:50 polyenantiomeric blend and the stereoblock polymer. This type of optical compensation has been described in other systems as an intercrystallite optical compensation. A detailed crystal structure analysis of these polymers is required to give insight into the structural compatibility of the polyenantiomorphs including helix sense. Work in this area is in progress and is expected to give direct evidence regarding an optically pure unit cell.

Acknowledgment. Financial support in the form of operating grants from the Natural Sciences and Engineering Research Council of Canada (NSERC) and the Québec Government (Fonds FCAR) is gratefully acknowledged. The authors are grateful to Drs. K. Patel and F. Sauriol for assistance in developing the polymerization techniques and for providing the ^{13}C NMR spectra, respectively, and to Ms. Norma Frangos for performing some of the radial growth rate measurements.

References and Notes

(1) Grenier, D.; Prud'homme, R. E.; Leborgne, A.; Spassky, N. *J. Polym. Sci., Polym. Chem. Ed.* **1981**, *19*, 1781.
(2) Grenier, D.; Prud'homme, R. E. *J. Polym. Sci., Polym. Phys. Ed.* **1984**, *22*, 577.
(3) Voyer, R.; Prud'homme, R. E. *Polym. Prepr. (Am. Chem. Soc., Div. Polym. Chem.)* **1988**, *29*, 611.
(4) Ritcey, A. M.; Prud'homme, R. E. *Macromolecules* **1992**, *25*, 972.
(5) Ritcey, A. M.; Brisson, J.; Prud'homme, R. E. *Macromolecules* **1992**, *25*, 2705.
(6) Ritcey, A. M.; Prud'homme, R. E. *Macromolecules* **1993**, *26*, 1376.
(7) Okihara, T.; Tsuji, M.; Kawaguchi, A.; Katayama, K.-I.; Tsuji, H.; Hyon, S.-H.; Ikoda, Y. *J. Macromol. Sci., Phys.* **1991**, *B30*, 119.
(8) Tsuji, H.; Ikada, Y. *Macromolecules* **1993**, *26*, 6918 and previous articles in this series.
(9) Liquori, A. M.; Anzuino, G.; Corio, V. M.; D'Alagni, M.; De Santis, P.; Savino, M. *Nature* **1965**, *206*, 358.
(10) Okihara, T.; Tsuji, M.; Kawaguchi, A.; Katayama, K.; Tsuji, H.; Hyon, S.-H.; Ikada, Y. *J. Macromol. Sci., Phys.* **1991**, *B30*, 119.
(11) Marega, C.; Marigo, A.; Di Noto, V.; Zannetti, R. *Makromol. Chem.* **1992**, *193*, 1599.
(12) Kovacs, A. J.; De Santis, P. *Biopolymers* **1968**, *6*, 299.
(13) Hoogsteen, W.; Postema, A. R.; Pennings, A. J.; ten Brinke, G.; Zugenmaier, P. *Macromolecules* **1990**, *23*, 634.
(14) Dumas, P.; Spassky, N.; Sigwalt, P. *Makromol. Chem.* **1972**, *156*, 55.
(15) Matsubayashi, H.; Chatani, Y.; Tadokoro, H.; Dumas, P.; Spassky, N.; Sigwalt, P. *Macromolecules* **1977**, *10*, 996.
(16) Sakakihara, H.; Takahashi, Y.; Tadokoro, H.; Oguni, N.; Tani, H. *Macromolecules* **1973**, *6*, 205.
(17) Yokouchi, M.; Chatani, Y.; Tadokoro, H.; Teranishi, K.; Tani, H. *Polymer* **1973**, *14*, 267.
(18) Okamura, K.; Marchessault, R. H. In *Conformation of Biopolymers*; Ramachandran, G. N., Ed.; Academic: London, 1967; Vol. 2, p 709.
(19) Sakakihara, H.; Takahashi, Y.; Tadokoro, H.; Sigwalt, P.; Spassky, N. *Macromolecules* **1969**, *2*, 515.
(20) Bloembergen, S.; Holden, D. A.; Bluhm, T. L.; Hamer, G. K.; Marchessault, R. H. *Macromolecules* **1989**, *22*, 1656.
(21) Bloembergen, S.; Holden, D. A.; Bluhm, T. L.; Hamer, G. K.; Marchessault, R. H. *Macromolecules* **1989**, *22*, 1663.
(22) Yokouchi, M.; Chatani, Y.; Tadokoro, H.; Tani, H. *Polym. J.* **1974**, *6*, 248.
(23) Takahashi, Y.; Tadokoro, H.; Hirano, T.; Sato, A.; Tsuruta, T. *J. Polym. Sci., Polym. Phys. Ed.* **1975**, *13*, 285.
(24) Natta, D. G.; Corradini, P.; Dall'Asta, G. *Atti Accad. Naz. Lincei, Cl. Sci. Fis., Mat. Nat., Rend.* **1956**, *20*, 408.
(25) Shambelan, C.; Hughes, R. E. *Natl. Meet.–Am. Chem. Soc.* **1958**.
(26) Stanley, E.; Litt, M. *J. Polym. Sci.* **1960**, *43*, 453.
(27) Cesari, M.; Perego, G.; Marconi, W. *Makromol. Chem.* **1966**, *94*, 194.
(28) Richards, J. R. Ph.D. Thesis, University of Pennsylvania, Philadelphia, 1961. *Diss. Abstr.* **1961**, *22*, 1029.
(29) Perego, G.; Cesari, M. *Makromol. Chem.* **1970**, *133*, 133.
(30) Hughes, R. E.; Cella, R. J. *Polym. Prepr. (Am. Chem. Soc., Div. Polym. Chem.)* **1974**, *15*, 137.
(31) Zmudzinski, L.; Sokol, M.; Turska, E. *Acta Polym.* **1985**, *36*, 483.
(32) Magill, J. H. *Makromol. Chem.* **1965**, *86*, 283.
(33) Dreyfuss, P. *ACS Symp. Ser.* **1975**, *6*, 70.
(34) Vandenberg, E. J. In *Macromolecular Synthesis*; Bailey, W. J., Ed.; Wiley: New York, 1972; Vol. 4, p 49.
(35) Cheng, H. N.; Smith, D. A. *J. Appl. Polym. Sci.* **1987**, *34*, 909.
(36) Steller, K. E. *ACS Symp. Ser.* **1975**, *6*, 136.
(37) Dworak, A. *Makromol. Chem. Rapid Commun.* **1985**, *6*, 665.
(38) Lindfors, K. R.; Pan, S.; Dreyfuss, P. *Macromolecules* **1993**, *26*, 2919.
(39) Pearce, R.; Brown, G. R.; Marchessault, R. H. *Polymer* **1994**, *35*, 3984.
(40) Janeczek, H.; Trzebicka, B.; Turska, E. *Polym. Commun.* **1987**, *28*, 123.
(41) Hoffman, J. D.; Weeks, J. J. *J. Chem. Phys.* **1962**, *37*, 1723.
(42) Price, F. P. *J. Polym. Sci.* **1959**, *39*, 139.
(43) Keller, A. *J. Polym. Sci.* **1959**, *39*, 151.
(44) Fujiwara, Y. *J. Appl. Polym. Sci.* **1960**, *4*, 10.
(45) Bassett, D. C.; Hodge, A. M. *Polymer* **1978**, *19*, 469.
(46) Morra, B. S.; Stein, R. S. *J. Polym. Sci.* **1982**, *B20*, 2261.
(47) Keith, H. D.; Padden, F. J., Jr.; Russell, T. P. *Macromolecules* **1989**, *22*, 666.
(48) Scandola, M.; Ceccorulli, G.; Pizzoli, M.; Gazzano, M. *Macromolecules* **1992**, *25*, 1405.
(49) Nakafuku, C.; Sakoda, M. *Polym. J.* **1993**, *25*, 909.
(50) Li, W.; Yan, R.; Jiang, B. *Polymer* **1992**, *33*, 889.
(51) Morra, B. S.; Stein, R. S. *Polym. Eng. Sci.* **1984**, *24*, 311.
(52) Lindenmeyer, P. H.; Holland, V. F. *J. Appl. Phys.* **1964**, *35*, 55.
(53) Briber, R. M.; Khoury, F. *J. Polym. Sci., Polym. Phys.* **1993**, *B31*, 1253.
(54) Keith, H. D.; Padden, F. J., Jr. *J. Appl. Phys.* **1963**, *34*, 2409.
(55) Keith, H. D.; Padden, F. J., Jr. *Polymer* **1984**, *25*, 28.
(56) Hoffman, J. D.; Lauritzen, J. I., Jr. *J. Res. Natl. Bur. Stand.* **1961**, *A65*, 297.
(57) Mandelkern, L. *Crystallization of Polymers*; McGraw-Hill Co.: New York, 1964; Chapter 8, p 264.
(58) Hoffmann, J. D.; Davis, G. T.; Lauritzen, J. I., Jr. In *Treatise on Solid State Chemistry*; Hannay, N. B., Ed.; Plenum Press: New York, 1976; Vol. 3, Chapter 7.
(59) Hoffman, J. D. *Polymer* **1983**, *24*, 3.
(60) Hoffman, J. D.; Miller, R. L.; Marand, H.; Roitman, D. B. *Macromolecules* **1992**, *25*, 2221.
(61) Keith, H. D.; Padden, F. J., Jr. *J. Appl. Polym. Phys.* **1964**, *35*, 1286.
(62) Cheng, S. Z. D.; Barley, J. S.; Giusti, P. A. *Polymer* **1990**, *31*, 845.
(63) Janimak, J. J.; Cheng, S. Z. D.; Giusti, P. A.; Hsieh, E. T. *Macromolecules* **1991**, *24*, 2253.

MA941165T